

Scanning x-ray microdiffraction of optically manipulated liposomes

D. Cojoc,^{a),b)} E. Ferrari, V. Garbin,^{c)} and E. Di Fabrizio^{d)}

CNR-INFM, Laboratorio Nazionale TASC, Area Science Park—Basovizza, I-34012 Trieste, Italy

H. Amenitsch,^{a),e)} M. Rappolt, B. Sartori, and P. Laggner

Austrian Academy of Sciences, Institute of Biophysics and Nanosystems Research, A-8042 Graz, Austria

M. Burghammer and C. Riekel

European Synchrotron Radiation Facility (ESRF), B.P. 220, F-38043 Grenoble Cedex, France

(Received 19 October 2007; accepted 9 November 2007; published online 6 December 2007)

We show optical tweezers manipulation of individual micron-sized samples investigating at the same time their inner nanostructure by synchrotron diffraction experiments. The validity of this technique is demonstrated for clusters of multilamellar liposomes trapped in single and multiple positions in the optical path of a microfocused x-ray beam and analyzed in a microscanning mode. The signal to background ratio of the first order peak shows that single liposome measurements are feasible. Multiple trapping by means of diffractive optical elements is demonstrated as an effective manipulation tool for future x-ray diffraction studies of the interaction between different sample entities.

The third generation synchrotron radiation (SR) sources generate intense x-ray beams, which can be used as experimental probes in various areas of basic and applied research.¹ Their high spectral brightness has allowed the development of optics for focusing soft and hard x-rays to micron and submicron focal spots: refractive, diffractive, or capillary optics, Kirkpatrick-Baez (KB) mirrors, two-dimensional (2D) waveguides, and multilayers.²⁻⁷ These achievements have enabled x-ray imaging and diffraction experiments on small sample volumes ($< \mu\text{m}^3$) to resolve structural information on a length scale from small-molecule crystallography (~ 0.1 nm) to large proteins or supramolecular assemblies (~ 100 nm).^{8,9} SR microbeam represents an ideal *in situ* probe to study local transient phenomena using inkjet systems¹⁰ or conformational changes within microfluidic cells.^{11,12} A common feature of these experiments is the need to move the sample, fixed on its support, in front of the x-ray beam. Consequently, this limits the freedom degrees for sample orientation and manipulation and does not allow to study interactions between two independent objects in terms of mutual orientation or growth (e.g., single cell study, real time crystal growth).

On the other hand, since the first demonstration,¹³ optical tweezers (OT) has emerged as a powerful tool in micro-manipulation of a large variety of microparticles immersed in fluids.¹⁴⁻¹⁶ Since OT allows to apply calibrated forces measuring the displacement of the trapped object with nanometer precision, to trap and manipulate multiple objects in real time, it can be considered as a valuable tool for sample manipulation in SR experiments.

Here, we demonstrate the usefulness of OT in micro-small-angle-x-ray-scattering (micro-SAXS) experiments of

colloidal suspensions (specifically, lipid/water model systems). The chosen lamellar and inverse hexagonal lipid/water systems find wide applications, especially in the food and pharmaceutical industries. For instance, multilamellar vesicles serve as model systems to mimic cellular biomembranes, dispersed lipid/water systems such as hexosomes and cubosomes are used as drug carriers,¹⁷ and lipoplex particles (cationic lipid/DNA complexes) serve as efficient transfection vectors.¹⁸ However, such systems are usually studied only in bulk and, therefore, a technique that allows single particle studies would be of great help for a deeper understanding and improvement of these pharmaceutical vehicles.

We designed and implemented a custom OT microscope and set it up in front of the microfocused x-ray beam at the ID13 beamline of the ESRF, to perform micro-SAXS experiments. The setup is shown in Fig. 1. The sample cell (SC),

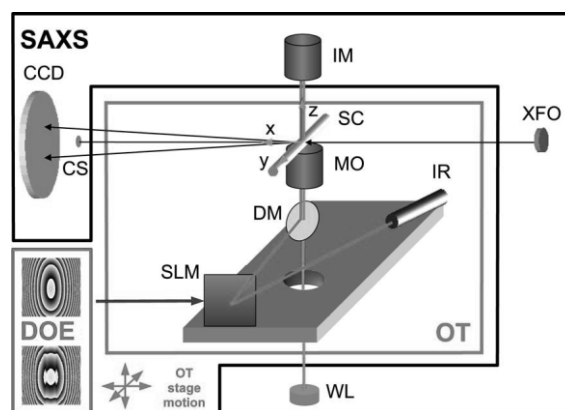


FIG. 1. (Color online) The combined SAXS-OT setup. The capillary SC, attached to the OT stage (red box), is illuminated by the WL source and observed by the IM, which are attached to the SAXS stage (black box). The x-ray beam is microfocused by x-ray focusing optics (XFO) inside the SC and the scattered light is recorded by the CCD. The IR laser beam is directed onto the spatial light modulator (SLM) and its wavefront shaped by DOEs (blue inset) to control the focus and the splitting of the beam which is then reflected to the microscope objective (MO) by the dichroic mirror DM. The laser beam is focused by the MO into the SC to form the trap. The OT stage can be moved along the three axes, as indicated by the red arrows.

^{a)}Authors to whom correspondence should be addressed.

^{b)}Electronic mail: cojoc@tasc.infm.it.

^{c)}Present address: Physics of Fluids, University of Twente, P.O. Box 217, 7500AE Enschede, The Netherlands.

^{d)}Also at: BIONEM Lab, University of Magna Græcia, V.le Europa 88100, Catanzaro, Italy.

^{e)}Electronic mail: amenitsch@elettra.trieste.it.

which contained the colloidal dispersions, was a thin walled glass capillary of 100/~80 μm external/internal diameters (Hilgenberg). By means of a remote controlled syringe pump (TSE Systems GmbH), small volumes of liquid were moved in front of the microfocussed x-ray beam. The direct beam was blocked by a central stop and the pattern of the x-ray light scattered by the sample was recorded with a 2D charge-coupled device (CCD) camera (MAR165, MarResearch). A white source and an upright microscope (objective 40X, Olympus) were used to image the sample. The SC holder and the OT microscope were built on a separate stage (red box in Fig. 1), which could be moved along the x , y and z axes to align the region of interest of the SC with the microfocussed x-ray beam. A single mode cw fiber laser (IPG-Photonics) generated a collimated linear polarized beam at 1064 nm. The phase of the wave front was controlled by a pre-calculated diffractive optical element (DOE), which was displayed onto the active area of the spatial light modulator (SLM) (PPM-X8267-11, Hamamatsu). The DOE allowed to suitably shape the laser beam, which was then directed by the dichroic mirror into the microscope objective [Nikon 60X, 0.7 numerical aperture (NA), dry] and focused into the SC to form the trap. The use of immersed objectives with high NA, typical for OT, was prevented because of the strong x-ray scattering induced by the immersion fluid touching the capillary. In addition, the capillary shape and the difference between the refractive indices of air, glass, and water made the capillary behave like a cylindrical lens which degraded the shape of the trap and, hence, its efficiency. This was compensated by using a spherical-cylindrical DOE (see the upper DOE in the blue inset of Fig. 1). Since the 0.7 NA of the trapping objective was low, the particles were trapped in two dimensions by the laser, the confinement in the third dimension being provided by the capillary wall. DOEs can also be used for multiple trapping.¹⁹ For instance, the DOE in the lower part of the blue inset in Fig. 1 shapes the laser beam to form two traps.

The monochromatic SR beam at 12.56 keV energy (0.987 Å wavelength) was focused onto the sample to about 1 μm^2 using KB mirror optics.³ The sample-to-detector distance was 348 mm and an Ag-behenate grain was used for calibration.²⁰ The imaging microscope (IM) was aligned to the grain's position, which was used as a reference thereafter (see the Cartesian reference system drawn in green in Fig. 1). The capillary, containing the colloidal dispersion, was then introduced into the setup to trap and fix the sample in the reference position. Lipid dispersions of palmitoyl-oleoyl- and di-oleoyl-phosphatidylethanolamine (POPE: multilamellar vesicles; DOPE: inverted hexagonal phase) (Avanti Polar Lipids) were prepared according to standard procedures in excess of water.²¹ Lipid concentrations were in the range of 0.1 – 1 mg/ml. The dispersion was transferred, at room temperature, into the capillary by the remotely controlled syringe pump. Using a laser power of 400 mW (at the exit of the laser), we created an optical trap of micrometric size where the POPE vesicles were attracted to form a cluster. The position of the OT stage was then adjusted to get the trapped cluster exactly in the focus of the IM.

A typical diffraction pattern of the POPE cluster, using 5 s exposure time is shown in Fig. 2. The exposure time was close to the limit of the radiation damage, as tested on a small cluster fixed to the capillary wall, but since only single exposures were taken in one position, the radiation damage

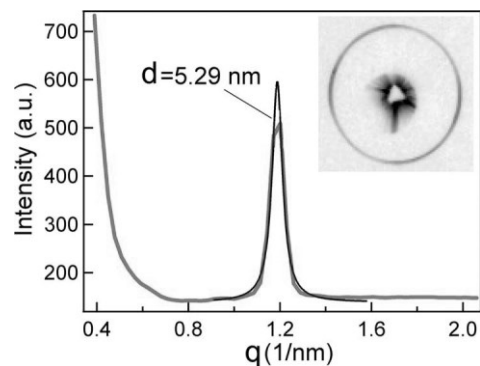


FIG. 2. (Color online) Plot of the azimuthally integrated intensity of a trapped POPE cluster (red line) and the Lorentzian function (black line) fitted to experimental data. The inset shows the 2D diffraction pattern as recorded by the CCD detector.

can be neglected for our experimental conditions. The radial intensity profile was obtained by azimuthally integrating the 2D diffraction pattern using the FIT2D software.²² The resulting d spacing of the first order diffraction peak $d = 5.29$ nm, corresponds well to the values obtained for bulk samples²³ showing that these specific experimental conditions do not affect the structure of the sample.

To demonstrate the capabilities of the technique, we performed a scanning diffraction experiment with a step size of $2.5 \times 5 \mu\text{m}^2$. Figure 3(b) shows a trapped cluster of POPE liposomes imaged by the IM. Some other small clusters attached to the capillary wall are also visible. To demonstrate that our cluster was not attached to the wall, we switched off the laser and saw the vesicles leaving the trap. Turning the laser on, the central cluster is formed again (see movie).²⁴ The corresponding scanning x-ray diffraction of the trapped POPE cluster, i.e., the first order intensity versus the scanning position, is shown in Fig. 3(c). From the Figs. 3(b) and 3(c), one can reconstruct the position and the shape of the trapped cluster inside the capillary, as shown in Fig. 3(d). Considering the full width half maximum intensity as relevant for size estimation, we assimilated the cluster to an ellipsoid, centered at about 12 μm below the capillary wall with the three main axes of about 10, 3, and 4 μm , respec-

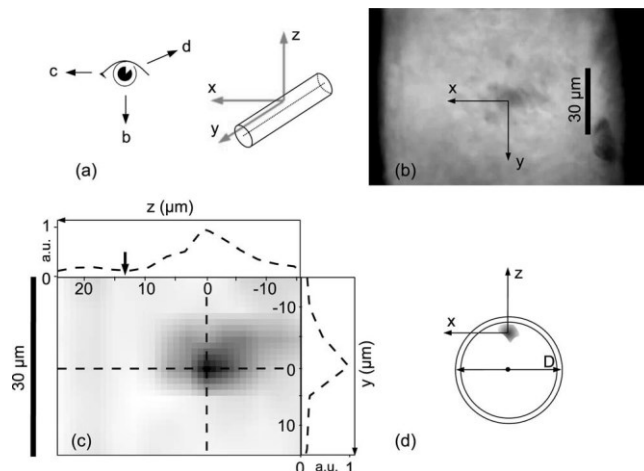


FIG. 3. Microcanning SAXS of an optically trapped POPE liposome cluster. (a) The three view points for the trapping region in capillary. (b) Optical image of the POPE cluster in the capillary. (c) X-ray diffraction image of the POPE cluster (the arrow indicates the capillary wall). (d) Transversal section of the capillary with the position of the trapped POPE cluster.

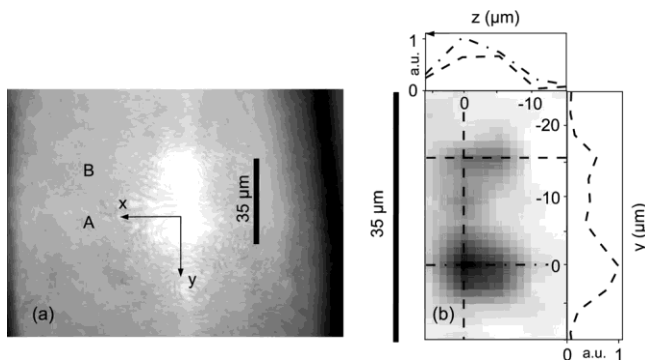


FIG. 4. Multiple trapping of DOPE clusters with an inverse hexagonal inner nanostructure. (a) Microscope image of the capillary with the IR-laser switched on, two laser traps are visible. (b) X-ray diffraction image of the two DOPE clusters, viewed in x direction.

tively. Since the size of the microfocused x-ray beam is $1 \mu\text{m}$ and the average size of POPE liposomes is about $1 \mu\text{m}$, we estimate that, at most, 10 liposomes got irradiated at once. Analyzing the values of the signal peak to background ratio (SPBR) $>450 / 1$ and scaling down the SPBR from 10 to 1 liposome, we conclude that single liposome measurements are feasible. Furthermore, the application of a more sensitive and fast CCD detector will help to reduce the exposure time to improve the SPBR and, hence, to reduce the radiation damage.

Another important remark is that, by using OT, the samples can not only be fixed and manipulated, their shape be analyzed (microscanning) and their inner nanostructure be determined (x-ray diffraction), but this technique allows also to change simultaneously the environmental conditions (e.g., pH, salinity) by remotely controlled microfluidics.

OT was demonstrated recently as a valuable technique to control the growth of birefringent tetragonal lysozyme crystals²⁵ and multiple trapping was used to investigate locally reactions on a micronscale using optical fluorescence microscopy.²⁶ Our technique allows to perform this type of experiments with x-ray beams. For instance, using two optical traps different micron-sized clusters, let us call them A and B, can be brought into contact and, consequently, a reaction between them can be induced. While OT is used to trigger the reaction, the combined microfocused x-ray beam would allow to view the nanostructural changes at the common interface of A and B. A proof of concept is illustrated in Fig. 4. Here, two microclusters of DOPE in the inverse hexagonal phase are fixed at about $15 \mu\text{m}$ from each other. The microscanning experiment (step width $3 \times 5 \mu\text{m}^2$) revealed one cluster (A) with an ellipsoidal shape (the longest axis, y of $\sim 10 \mu\text{m}$) and another cluster (B) with almost spherical shape (diameter of $\sim 10 \mu\text{m}$). The cluster B contains less lipid material than the cluster A since the flux of fluid is oriented down to top and, hence, the second trap is partially shielded by cluster A. In a second step, using a sequence of DOEs, the two DOPE entities can be brought close to each other and as a consequence fuse.

In this letter, we presented a combined setup that enables microdiffraction x-ray experiments of microsamples that are fixed and manipulated by means of OT inside a capillary which is connected to a remotely controlled microfluidic circuit. Single and multiple optical traps created by means of

DOEs are demonstrated for fixing the samples in scanning micro-SAXS experiments with multilamellar liposomes. The high SPBR for ten liposomes shows that single liposome measurements are feasible. Multiple trapping was demonstrated in the view of future more complex experiments, e.g., investigate the reactions between different colloidal microsystems.

The setup can be improved to enable three-dimensional optical trapping and simultaneous imaging through the same objective. In this regards, we are considering new immersion objectives, with long-working distance and high enough NA.

The results presented here have given insight into the very fascinating gamble field—to look at single supramolecular assemblies with micron- and submicron-sized SR beams, which will find multiple applications in third and in particular future fourth generation SR sources.

The authors thank Federico Salvador from TASC, Christian Morello from Synchrotron Elettra, and Lionel Lardiere from ID13 for their considerable technical support.

¹*Third-Generation Hard X-ray Synchrotron Radiation Sources: Source Properties, Optics, and Experimental Techniques*, edited by D. M. Mills (Wiley-Interscience, New York, 2002).

²I. McNulty, Proc. SPIE **2516**, 1 (1998).

³O. Hignette, P. Cloetens, W. K. Lee, W. Ludwig, and G. Rostaing, J. Phys. (France) **104**, 231 (2003).

⁴B. Noehammer, C. David, M. Burghammer, and C. Riekel, Appl. Phys. Lett. **86**, 163104 (2005).

⁵B. Lengeler, C. G. Schroer, J. Tümmeler, B. Benner, A. Gerhardus, T. F. Gunzler, M. Kuhlmann, J. Meyer, and G. Zimprich, J. Synchrotron Radiat. **9**, 119 (2002).

⁶F. Pfeiffer, C. David, M. Burghammer, C. Riekel, and T. Salditt, Science **297**, 230 (2002).

⁷C. Liu, R. Conley, A. T. Macrander, J. Maser, H. C. Kang, and G. B. Stephenson, Thin Solid Films **515**, 654 (2006).

⁸C. Riekel, Rep. Prog. Phys. **63**, 233 (2000).

⁹C. Riekel, M. Burghammer, and G. Schertler, Curr. Opin. Struct. Biol. **15**, 556 (2005).

¹⁰H. Lemke, M. Burghammer, D. Flot, M. Roessle, and C. Riekel, Biomacromolecules **5**, 1316 (2004).

¹¹L. Pollack, M. W. Tate, N. C. Darnton, J. B. Knight, S. M. Gruner, W. A. Eaton, and R. H. Austin, Proc. Natl. Acad. Sci. U.S.A. **96**, 10115 (1999).

¹²R. J. Davies, M. Burghammer, and C. Riekel, Appl. Phys. Lett. **87**, 264105 (2005).

¹³A. Ashkin and J. M. Dziedzic, Appl. Phys. Lett. **19**, 283 (1971).

¹⁴*Special issue on optical micromanipulation*, edited by N. Heckenberg and K. Dholakia, special issue of J. Opt. A, Pure Appl. Opt. **9** (2007).

¹⁵D. G. Grier, Nature (London) **424**, 810 (2003).

¹⁶K. C. Neuman and St. M. Block, Rev. Sci. Instrum. **75**, 2787 (2004).

¹⁷K. Larsson, Curr. Opin. Colloid Interface Sci. **4**, 64 (2000).

¹⁸I. Koltover, T. Salditt, J. O. Rädler, and C. R. Safinya, Science **281**, 78 (1998).

¹⁹E. R. Dufresne and D. G. Grier, Rev. Sci. Instrum. **69**, 1974 (1998).

²⁰T. C. Huang, H. Toraya, T. N. Blanton, and Y. J. Wu, J. Appl. Crystallogr. **26**, 180 (1993).

²¹D. D. Lasic, *Liposomes: From Physics to Applications* (Elsevier, Amsterdam, 1993).

²²A. Hammersley, see www.esrf.fr/computing/scientific/FIT2D/.

²³M. Rappolt, A. Hickel, F. Bringezu, and K. Lohner, Biophys. J. **84**, 3111 (2003).

²⁴See EPAPS Document No. E-APPLAB-91-086749 for liposome trapping in capillary (movie). This document can be reached via a direct link in the online article's HTML reference section or the EPAPS homepage (<http://www.aip.org/pubservs/epaps.htm>).

²⁵W. Singer, H. Rubinsztein-Dunlop, and U. Gibson, Opt. Express **12**, 6440 (2004).

²⁶S. Kulin, R. Kishore, K. Helmersson, and L. Locascio, Langmuir **19**, 8206 (2003).